ORIGINAL SCIENTIFIC PAPER

CROATICA CHEMICA ACTA

Croat. Chem. Acta **2025**, *98*(4), 289–297
Published online: January 15, 2026
DOI: 10.5562/cca4162

HKD 1926

On the Double-Stranded DNA Model by Using an Analytical Method in Soliton Theory

Wei Gao,[1] Haci Mehmet Baskonus[2,*]

[1] School of Mathematics, Hohai University, Nanjing 211100, China
[2] Faculty of Education, Harran University, Sanliurfa 63150, Turkey
* Corresponding author's e-mail address: hmbaskonus@gmail.com

RECEIVED: June 01, 2025 ✯ REVISED: November 26, 2025 ✯ ACCEPTED: November 26, 2025

Abstract: In this work, with the aid of computational program, the modified exp[−Ω(ξ)]-expansion function method (MEFM) is considered to obtain some new results to the double-stranded Deoxyribonucleic acid (DNA) model. We extract some new complex polynomial and soliton solutions to the governing system of equations. Moreover, we plot 2D and 3D graphical distributions of dependant variable of the double stranded DNA model.

Keywords: the double-stranded DNA model, the MEFM, complex function, hyperbolic function structures.

INTRODUCTION

TODAY, modern technology has rendered possible better understanding the problems of daily life. During its process, this technology has used the basic properties of interdisciplinary fields. At the first glance, mathematical norms from trigonometric properties to special functions have been plaid an important role. Especially, modern tools such as deep learning, machine learning and artificial intelligence [1–3] have been considered. Many experts have benefited from these items to investigate these problems such as health diseases and natural problems, especially, DNA problems caused by genetic diseases. Deep learning tool has been used to observe the identification of DNA-binding proteins.[4] More recently, Ward and their team worked on DNA-damageassociated protein.[5] Caldecott studied on DNA single-strand break repair by using dynamic networks.[6] They observed that protein connection in DNA-damage-associated influences the tolerance to genetic variation. A genetical study of DNA sequence structures and DNA repair gene variant was conducted by Monckton and his team.[7] Nikjoo and his team studied on the mechanistic modelling studies of DNA damage and DNA repair.[8] Recently, the mathematical models of DNA methylation dynamics were introduced to the literature to observe the incorporation of hydroxymethylation[9] which was observed the global methylome and then to local epigenetic regions.

In this study, we observe the double-stranded DNA model which is based on partial differential equations (PDEs),[10–12]

$$\begin{aligned} &u_{tt} - c_1^2 u_{xx} - c_1^2 u_{yy} - c_1^2 u_{zz} - \\ &\Lambda_1 u - \Gamma_1 uv - \Omega_1 u^3 - \Omega_3 uv^2 = 0, \\ &v_{tt} - c_2^2 v_{xx} - c_2^2 v_{yy} - c_2^2 v_{zz} - \\ &\Lambda_2 v - \Gamma_2 u^2 - \Omega_2 u^2 v - \Omega_4 v^3 + c_0 = 0, \end{aligned} \tag{1}$$

in which $u = u(x,y,z,t), v = v(x,y,z,t)$ represent the variation in longitudinal displacements between the bottom and top strings, symbolise their transverse motion, respectively. The constants used in Eq. (1) being c_1, c_2, Λ_1, Λ_2, Γ_1, Γ_2, Ω_1, Ω_2, Ω_3, Ω_4 and c_0 are defined as follows

$$\begin{aligned} &c_1 = \pm\frac{\varepsilon}{\rho_1},\ c_2 = \pm\frac{F}{\rho_1},\ \Lambda_1 = \frac{-2\mu_1}{\rho_1\sigma_1 h}\left(c - L_0\right), \\ &\Omega_3 = \Omega_4 = \frac{4\mu_1 L_0}{\rho_1\sigma_1 h^3},\ \Gamma_1 = 2,\ c_0 = \frac{\sqrt{2}\mu_1\left(h - L_0\right)}{\rho_1\sigma_1}, \\ &\Lambda_2 = \frac{-2\mu_1}{\rho_1\sigma_1},\ \Gamma_2 = \frac{2\sqrt{2}\mu_1 L_0}{\rho_1\sigma_1 h^2},\ \Omega_1 = \Omega_2 = \frac{-2\mu_1 L_0}{\rho_1\sigma_1 h^3}, \end{aligned} \tag{2}$$

This work is licensed under a Creative Commons Attribution 4.0 International License.

where ρ_1 denotes the mass density, σ_1 represents the transverse cross-sectional area of the strand. The parameter corresponds to Young's modulus, and F defines the tension per unit length within the strand. The rigidity of the elastic membrane is given by μ_1, h denotes the distance separating the two DNA strands, and L_0 represents the membrane's equilibrium height. Eq. (1) was studied by Elmandouh and his team in x and t domain.[13] In their work, the complete discrimination and direct method were used to extract some results in solitary, periodic, kink, and singular solutions. Moreover, Kumar et al introduced to literature the solitonic structures of DNA in x and t domain.[14]

The paper is divided into five sections. Section 2 provides an overview of the proposed MEFM. Section 3 demonstrates the new results of our method on the double-stranded DNA model and provides some physical simulations of the new solutions. Section 4 includes some important future for the doublestranded DNA model and approach. Section 5 offers a conclusive overview of this manuscript.

PRELIMINARIES OF SCHEME

In this part of the manuscript, we introduce the main properties of the MEFM in detail as the following steps:

Step 1: Let's consider a general PDEs given as

$$P\left(u,\ u_x,\ u_{xx},\ u_{xxt},\ u_x u^2,\cdots\right)=0 \tag{3}$$

in which $u = u(x,t)$ is unknown function, P is a polynomial of $u(x,t)$ together with its derivatives. We convert Eq.(3) by using the wave transformation formula given as

$$u\left(x,t\right)=U\left(\xi\right),\ \ \xi=kx-ct,\ \ k\neq 0,\ \ c\neq 0, \tag{4}$$

into the nonlinear ordinary differential equation (NODE) obtained as

$$NODE\left(U,U',U'',U^2,\cdots\right)=0, \tag{5}$$

being NODE is a polynomial of $U = U(\xi)$ and its derivatives such as $U' = dU / d\xi$, $U'' = d^2U / d\xi^2$.

Step 2: In this second step, we consider the wave solution formula of Eq.(5) in following format

$$U\left(\xi\right)=\frac{\sum_{i=o}^{N}A_i\left[e^{-\Omega\left(\xi\right)}\right]^i}{\sum_{j=0}^{M}B_j\left[e^{-\Omega\left(\xi\right)}\right]^j}, \tag{6}$$

being $A_i, B_j, (0 \le i \le N,\ 0 \le j \le M)$ are constants to be determined later, such that $A_N \neq 0$, $B_M \neq 0$. M and N are positive integers via obtained by using the homogeneous balance principle. In Eq.(6), $\Omega = \Omega(\xi)$ satisfies the following differential equation

$$\Omega'\left(\xi\right)=e^{-\Omega\left(\xi\right)}+\mu e^{\Omega\left(\xi\right)}+\lambda. \tag{7}$$

Eq.(7) has many solutions, but here, we consider several of such families of these solutions [15,16] as follows:

Family 1: When $\mu \neq 0$, $\lambda^2 - 4\mu > 0$,

$$\Omega\left(\xi\right)=\ln\left(\frac{-\sqrt{\lambda^2-4\mu}}{2\mu}\tanh\left(\frac{\sqrt{\lambda^2-4\mu}}{2}\left(\xi+E\right)\right)-\frac{\lambda}{2\mu}\right) \tag{8}$$

Family 2: When $\mu \neq 0$, $\lambda^2 - 4\mu < 0$,

$$\Omega\left(\xi\right)=\ln\left(\frac{\sqrt{-\lambda^2+4\mu}}{2\mu}\tan\left(\frac{\sqrt{-\lambda^2+4\mu}}{2}\left(\xi+E\right)\right)-\frac{\lambda}{2\mu}\right) \tag{9}$$

Family 3: When $\mu \neq 0$, $\lambda \neq 0$ and $\lambda^2 - 4\mu > 0$

$$\Omega\left(\xi\right)=-\ln\left(\frac{\gamma}{e^{\lambda\left(\xi+E\right)}-1}\right) \tag{10}$$

Family 4: When $\mu \neq 0$, $\lambda \neq 0$ and $\lambda^2 - 4\mu = 0$

$$\Omega\left(\xi\right)=\ln\left(-\frac{2\lambda\left(\xi+E\right)+4}{\lambda^2\left(\xi+E\right)}\right) \tag{11}$$

Family 5: When $\mu = 0$, $\lambda = 0$ and $\lambda^2 - 4\mu = 0$

$$\Omega\left(\xi\right)=\ln\left(\xi+E\right) \tag{12}$$

in which $A_i, B_i, (0 \le i \le N,\ 0 \le j \le M)$ and E are coefficients to be determined later.

Step 3: In this step, we calculate the coefficients of Eq.(6). If we insert Eq.(6) and its derivatives together with Eq.(7) into Eq.(5), we obtain a system of equations involving polynomial of $e^{-\Omega(\xi)}$. Solving this system by using various computational programs, we reach the values of coefficients A_i, B_i, E, λ, μ, k, c. Putting these values of the coefficients along with one of Eqs.(8–12) into Eq. (6), we obtain various new solutions to the Eq.(3).

APPLICATIONS

In this sub-section of the manuscript, the MEFM is used to extract various special complex solutions of the double-stranded DNA model. If we use the travelling wave transformation defined by $u = U(\xi)$, $v = V(\xi)$, $\xi = mx + ny + rz - kt$ where $m \neq 0$, $n \neq 0$, $r \neq 0$, $k \neq 0$, into Eq.(1), we convert it to the following NODE

$$\tau_1 U'' - \tau_2 U - \tau_3 U^2 - \tau_4 U^3 = 0 \tag{13}$$

in which $V = \alpha U + \beta$ and also $\tau_1 = k^2 - c_1^2 m^2 - c_1^2 n^2 - c_1^2 r^2$, $\tau_2 = \Lambda_1 + \Gamma_1\beta + \Omega_3\beta^2$, $\tau_3 = \alpha\Gamma_1 + 2\alpha\beta\Omega_3$, $\tau_4 = \Omega_1 + \alpha^2\Omega_3$, $c_1 = c_2$, $\Lambda_2 = \Lambda_1 + \Gamma_1\beta + \Omega_3\beta^2 - 3\Omega_4\beta^2$, $\Gamma_2 = \alpha^2\Gamma_1 + 2\alpha^2\beta\Omega_3 - 3\Omega_4\alpha^2\beta - \Omega_2\beta$, $\Omega_4 = \Omega_1 + \alpha^2\Omega_3 - \Omega_2$, $c_0 = -\Omega_4\beta^3 - \beta\Lambda_2$.

Via balance rule on Eq.(13), we find a relationship N and M as below:

$$N = M + 1 \tag{14}$$

in which $N, M \in Z^+$. According to various values of N and M, we extract following cases.

Case 1: When we take the basic values of N and M as $M = 1$, $N = 2$ for Eq.(6), we may write the test function of the solution formula for Eq.(13) as follows

$$U(\xi) = \frac{A_0 + A_1 e^{-\Omega(\xi)} + A_2 e^{-2\Omega(\xi)}}{B_0 + B_1 e^{-\Omega(\xi)}} = \frac{\Psi}{\Upsilon} \tag{15}$$

where $B_1 \neq 0$. For Eq.(13), we need to take second derivations [Eq.(15)]. So, we find it as follows

$$U'(\xi) = \frac{\Psi'\Upsilon - \Psi\Upsilon'}{\Upsilon^2} = \frac{\Delta}{\Theta} \quad \text{and} \quad U''(\xi) = \frac{\Delta'\Theta - \Delta\Theta'}{\Theta^2} \tag{16}$$

If we substitute Eq.(15) and Eq.(16) into Eq.(13), we find a polynomial of $e^{-\Omega(\xi)}$. Solving this equations with aid of various computational programs and extract the values of the coefficients. To gain some new solutions for Eq.(1), we consider each case given by follows

Case 1.1: Under the Family-1 conditions, if we select following coefficients

$$\alpha = 1,\ c_1 = c_2,\ \Omega_4 = \alpha^2\Omega_3 + \Omega_1 - \Omega_2,\ B_0 = 3,\ A_1 = 2,\ B_1 = 1,\ A_2 = 1,\ \beta = 2,\ \Gamma_2 = -3\alpha^2\beta\Omega_4 + 2\alpha^2\beta\Omega_3 + \alpha^2\Gamma_1 - \beta\Omega_2,\ \Lambda_2 = \beta^2\Omega_3 - 3\beta^2\Omega_4 + \beta\Gamma_1 + \Lambda_1,\ c_0 = -\beta^3\Omega_4 - \beta\Lambda_2, n = i,\ \Lambda_1 = -i,\ \Omega_3 = 3,\ \Gamma_1 = 2, A_0 = B_0(2 - B_0),$$

$$\Omega_1 = \left(-\frac{667}{2313} + \frac{392i}{2313}\right)\alpha^2, \lambda = 4 + \frac{\left(\frac{24}{7} - \frac{3i}{14}\right)}{\alpha} - 2B_0,$$

$$k = -\frac{i(2 - 2B_0)^{3/2}\sqrt{196\alpha^2 + (144 - 9i)c_1^2(m^2 + r^2 - 1)}}{3\sqrt{(16 - i)(2B_0 - 2)^3}}$$

$$\mu = \frac{(B_0 - 2)(14\alpha B_0 + (-28\alpha - (48 - 3i)))}{14\alpha}$$

we find the following complex trigonometric function solution as

$$u_{1,1(x,y,z,t)} = -1 - \frac{\frac{34}{7} - \frac{3i}{7}}{-\frac{10}{7} + \frac{3i}{14} + \left(\frac{3}{14} + \frac{24i}{7}\right)\tan(f(x,y,z,t))} \tag{17}$$

where

$$f(x,y,z,t) = \left(\frac{3}{28} + \frac{12i}{7}\right)\left(\frac{t\sqrt{196 + (144 - 9i)c_2^2(m^2 + r^2 - 1)}}{3\sqrt{16 - i}} + E + mx + rz + iy\right)$$

The graphical simulations of $u_{1,1}(x,y,z,t)$ are plotted in Figure 1.

Case 1.2. In this case, we consider two family conditions given by Eq.(8) and Eq.(9) as following cases.

Case 1.2.1: With the conditions of the Family-1, when we select these

$$c_1 = c_2,\ \Omega_4 = \alpha^2\Omega_3 + \Omega_1 - \Omega_2,\ \alpha = 1,\ A_1 = 2,\ B_0 = 3,\ A_1 = 2,\ B_1 = 1,\ \Gamma_2 = -3\alpha^2\beta\Omega_4 + 2\alpha^2\beta\Omega_3 + \alpha^2\Gamma_1 - \beta\Omega_2,\ A_2 = 1,\ \beta = 2,\ n = i,\ \Lambda_1 = -i,\ \Omega_3 = 3,$$

$$\Lambda_2 = \beta^2\Omega_3 - 3\beta^2\Omega_4 + \beta\Gamma_1 + \Lambda_1,\ c_0 = \beta^3(-\Omega_4) - \beta\Lambda_2,\ \Gamma_1 = 2,$$

$$\lambda = A_1,\ A_0 = \frac{14\alpha A_1^2 + (48 - 3i)A_1B_1 - (96 - 6i)B_0}{56\alpha},$$

$$\Omega_1 = \frac{\alpha(B_1(9\alpha A_1 + 28B_1) - 18\alpha B_0)}{6B_0 - 3A_1B_1},$$

$$k = \frac{\sqrt{\frac{16}{3} - \frac{i}{3}}(A_1B_1 - 2B_0)\sqrt{14\alpha + 3c_1^2(2B_0 - A_1B_1)(m^2 + r^2 - 1)}}{\sqrt{(16 - i)(2B_0 - A_1B_1)^3}},$$

$$\mu = \frac{14\alpha A_1^2 + (48 - 3i)A_1B_1 - (96 - 6i)B_0}{56\alpha},$$

we find the following complex hyperbolic function solution as

$$u_{2,1} = \frac{\frac{-68}{7} + \frac{6i}{7}}{-2 - \sqrt{\frac{96}{7} - \frac{6i}{7}}\tanh(f)} + \frac{\frac{1147}{49} - \frac{204i}{49}}{\left(-2 - \sqrt{\frac{96}{7} + \frac{6i}{7}}\tanh(f)\right)^2} + \left(-\frac{17}{7} + \frac{3i}{14}\right) \Bigg/ \left(3 - \frac{\frac{34}{7} - \frac{3i}{7}}{-2 - \sqrt{\frac{96}{7} - \frac{6i}{7}}\tanh(f)}\right) \tag{18}$$

where

$$u_{2,1} = u_{2,1}(x,y,z,t),\ f = f(x,y,z,t) = \sqrt{\frac{24}{7} + \frac{3i}{14}}(\varpi t + E + mx + rz + iy),$$

$$\varpi = \frac{\sqrt{12c_2^2(m^2 + r^2 - 1) + 14}}{2\sqrt{3}}.$$

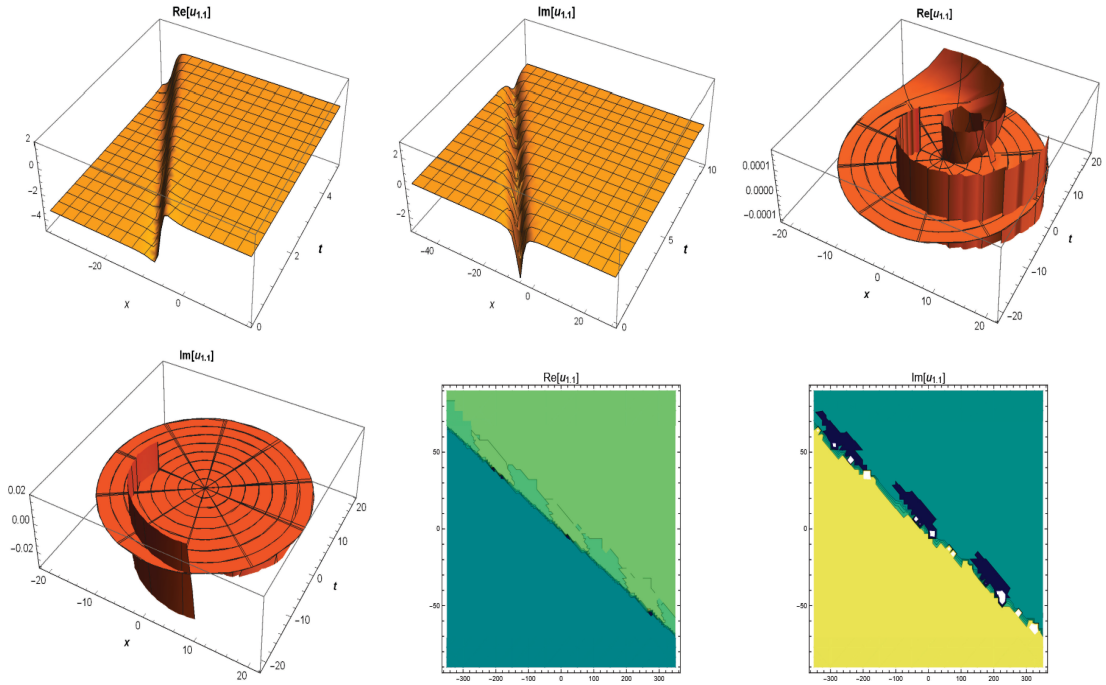

Figure 1. The 3D, revolution and contour surfaces of Eq.(17).

The graphical simulations of $u_{2,1}(x,y,z,t)$ are seen in Figure 2.

Case 1.2.2. With the conditions of the Family 2, selecting

$$\alpha = 1,\ A_1 = 2,\ B_0 = 3,\ B_1 = 1,\ A_2 = 1,\ \beta = 2,\ n = i,\ \Lambda_1 = -i,\ \Omega_3 = 3,$$
$$\Gamma_1 = 2, A_0 = \frac{14\alpha A_1^2 + (48 - 3i)A_1B_1 - (96 - 6i)B_0}{56\alpha},$$
$$\Omega_1 = \frac{\alpha\left(B_1(9\alpha A_1 + 28B_1) - 18\alpha B_0\right)}{6B_0 - 3A_1B_1},$$
$$k = \frac{\sqrt{\frac{16}{3} + \frac{i}{3}}\,(A_1B_1 - 2B_0)\sqrt{14\alpha + 3c_1^2(2B_0 - A_1B_1)\left(m^2 + r^2 - 1\right)}}{\sqrt{(16 - i)(2B_0 - A_1B_1)^3}},$$
$$\lambda = A_1,\ \mu = \frac{14\alpha A_1^2 + (48 - 3i)A_1B_1 - (96 - 6i)B_0}{56\alpha},\ c_1 = c_2,$$
$$\Lambda_2 = \beta^2\Omega_3 - 3\beta^2\Omega_4 + \beta\Gamma_1 + \Lambda_1,$$
$$\Gamma_2 = -3\alpha^2\beta\Omega_4 + 2\alpha^2\beta\Omega_3 + \alpha^2\Gamma_1 - \beta\Omega_2,$$
$$\Omega_4 = \alpha^2\Omega_3 + \Omega_1 - \Omega_2,\ c_0 = \beta^3(-\Omega_4) - \beta\Lambda_2$$

we find the following complex hyperbolic function solution as

$$u_{2,2} = \frac{-\frac{17}{7} + \frac{3i}{14} + \frac{-\frac{68}{7} + \frac{6i}{7}}{-2 + \sqrt{-\frac{96}{7} + \frac{6i}{7}}\tan(f)} + \frac{\frac{1147}{49} - \frac{204i}{49}}{\left(-2 + \sqrt{-\frac{96}{7} + \frac{6i}{7}}\tan(f)\right)^2}}{3 - \frac{\frac{34}{7} - \frac{3i}{7}}{-2 + \sqrt{-\frac{96}{7} + \frac{6i}{7}}\tan(f)}} \quad (19)$$

where

$$u_{2,2} = u_{2,2}(x,y,z,t),\ f = f(x,y,z,t) = \sqrt{-\frac{24}{7} + \frac{3i}{14}}\,(E + mx + iy + rz + \varsigma t),$$
$$\varsigma = \frac{\sqrt{12c_2^2(m^2 + r^2 - 1) + 14}}{2\sqrt{3}}.$$

The graphical simulations of $u_{2,2}(x,y,z,t)$ are seen in Figure 3.

Case 1.3: Via the Family-1 conditions, considering follows

$$\Lambda_2 = \beta^2\Omega_3 - 3\beta^2\Omega_4 + \beta\Gamma_1 + \Lambda_1,\ \Gamma_2 = -3\alpha^2\beta\Omega_4 + 2\alpha^2\beta\Omega_3 + \alpha^2\Gamma_1 - \beta\Omega_2,$$
$$\Omega_4 = \alpha^2\Omega_3 + \Omega_1 - \Omega_2,\ c_0 = \beta^3(-\Omega_4) - \beta\Lambda_2,\ m = 1,\ r = 2,\ B_1 = 3,$$
$$\Omega_1 = 2,\ B_0 = 2,\ \alpha = 1,\ c_2 = 1,\ A_2 = 1,\ \beta = 2,\ n = i,\ \Lambda_1 = -i,\ \Omega_3 = 3,$$
$$\Gamma_1 = 2,\ A_0 = \frac{-56\alpha B_0 - (48 - 3i)B_1^2}{6(3\alpha^2 + \Omega_1)} + \frac{196\alpha^2B_1^2}{9(3\alpha^2 + \Omega_1)^2} + \frac{B_0^2}{B_1^2},$$
$$A_1 = \frac{2B_0}{B_1} - \frac{28\alpha B_1}{3(3\alpha^2 + \Omega_1)},\ \mu = \frac{-56\alpha B_0 - (48 - 3i)B_1^2}{6(3\alpha^2 + \Omega_1)} + \frac{196\alpha^2B_1^2}{9(3\alpha^2 + \Omega_1)^2} + \frac{B_0^2}{B_1^2},$$
$$k = -\frac{\sqrt{3\alpha^2 + 2B_1^2c_1^2(m^2 + r^2 - 1) + \Omega_1}}{\sqrt{2}B_1},\ \lambda = \frac{2B_0}{B_1} - \frac{28\alpha B_1}{3(3\alpha^2 + \Omega_1)},\ c_1 = c_2,$$

We find another complex trigonometric function solution as

$$u_{3,1} = \frac{\frac{283648}{3375} - \frac{192i}{25} + \frac{\frac{19478599}{50625} - \frac{8864i}{125}}{\left(\frac{64}{15} - 3\sqrt{\frac{32}{5} - \frac{2i}{5}}\tanh(f)\right)^2} - \frac{2216}{225} + \frac{9i}{10}}{2 - \frac{\frac{4432}{75} - \frac{27i}{5}}{\frac{64}{15} - 3\sqrt{\frac{32}{5} - \frac{2i}{5}}\tanh(f)}}, \quad (20)$$

where

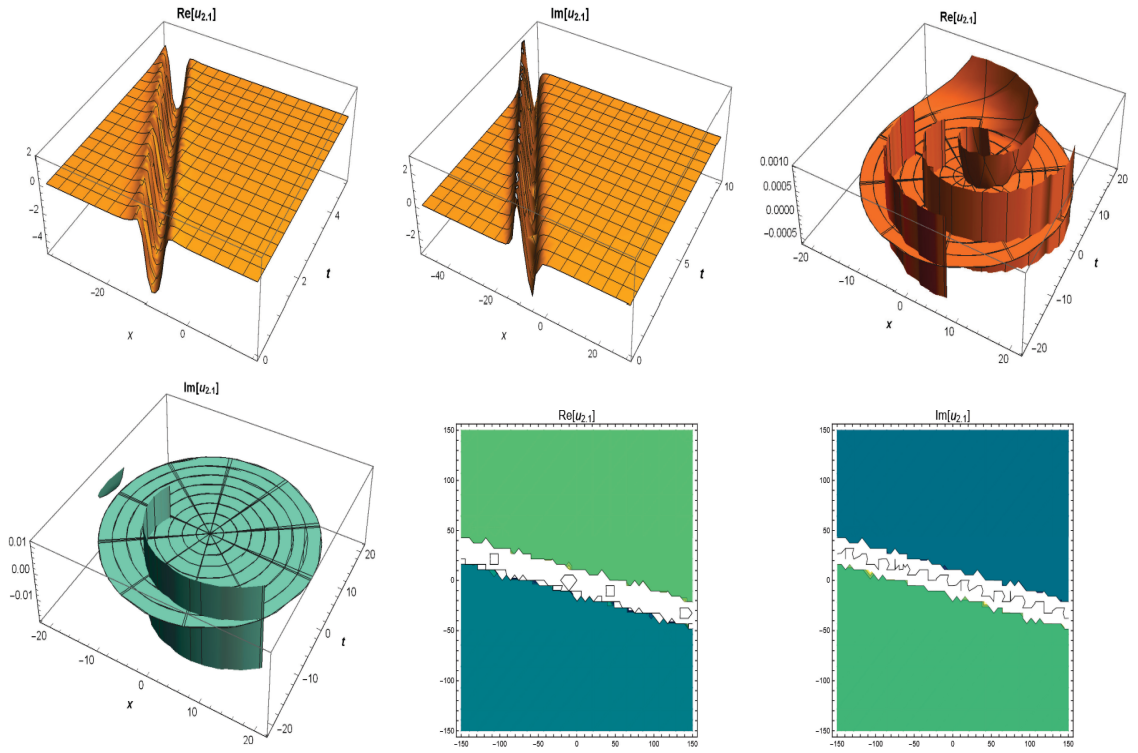

Figure 2. The 3D, revolution and contour surfaces of Eq. (18).

$$u_{3,1} = u_{3,1}(x,y,z,t), f = f(x,y,z,t) = 3\sqrt{\frac{8}{5} - \frac{i}{10}}\left(E + \frac{1}{3}\sqrt{\frac{77}{2}}t + x + iy + 2z\right).$$

The graphical simulations of $u_{3,1}(x,y,z,t)$ are plotted in Figure 4.

Case 2: When we take as $M = 2$, $N = 3$ for Eq.(6), we may write the test function of the solution formula for Eq.(13) as follows.

$$U(\xi) = \frac{A_0 + A_1 e^{-\Omega(\xi)} + A_2 e^{-2\Omega(\xi)} + A_3 e^{-3\Omega(\xi)}}{B_0 + B_1 e^{-\Omega(\xi)} + B_2 e^{-2\Omega(\xi)}} = \frac{\Psi}{\Upsilon}. \quad (21)$$

Putting Eq.(21) and its second derivative into the Eq.(13), we extract following complex polynomial solutions.

Case 2.1: Selecting follows together with Family-4 conditions

$$A_3 = i,\ A_1 = A_2 = B_1 = 0,\ \beta = 1,\ n = i,$$
$$\Omega_3 = 1,\ \Lambda_1 = -i,\ \Gamma_1 = 2,$$
$$\Omega_1 = B_0 = 1,\ A_0 = \frac{-1}{3}\sqrt{1 + \frac{i}{2}},\ B_2 = -\left(-\frac{4}{5} + \frac{2i}{5}\right)^{\frac{1}{3}} 3^{\frac{2}{3}},$$
$$\alpha = -\sqrt{1 - 2i},\ \lambda = \frac{2(-2-i)^{\frac{1}{6}} 2^{\frac{5}{6}}}{3^{\frac{1}{3}}},$$
$$k = \frac{-1}{3}\sqrt{\frac{3-i}{10}}\sqrt{(-4+2i)^{\frac{1}{3}} 15^{\frac{2}{3}} + (27+9i)(-1+m^2+r^2)c_1^2},$$
$$\mu = 2(-2-i)^{\frac{1}{3}}\left(\frac{2}{3}\right)^{\frac{2}{3}},\ \Lambda_2 = \beta^2\Omega_3 - 3\beta^2\Omega_4 + \beta\Gamma_1 + \Lambda_1,$$
$$\Gamma_2 = -3\alpha^2\beta\Omega_4 + 2\alpha^2\beta\Omega_3 + \alpha^2\Gamma_1 - \beta\Omega_2,$$
$$\Omega_4 = \alpha^2\Omega_3 + \Omega_1 - \Omega_2,\ c_1 = c_2,\ c_0 = \beta^3(-\Omega_4) - \beta\Lambda_2$$

we find the following complex polynomial solution

$$u_{4,1} = -\frac{1}{3}\sqrt{1 + \frac{i}{2}} - \frac{\sigma(E + mx + iy + rz + \Phi t)^3}{\left(4 + \frac{4(-2-i)^{\frac{1}{6}} 2^{\frac{5}{6}} (E + mx + iy + rz + \Phi t)^3}{3^{\frac{1}{3}}}\right)^3} \Bigg/ 1 - \frac{\varsigma(E + mx + iy + rz + \Phi t)^2}{3^{\frac{2}{3}}\left(4 + \frac{4(-2-i)^{\frac{1}{6}} 2^{\frac{5}{6}} (E + mx + iy + rz + \Phi t)^3}{3^{\frac{1}{3}}}\right)^2} \quad (22)$$

where

$$u_{4,1} = u_{4,1}(x,y,z,t),\ \sigma = \frac{2048}{9} - \frac{4096i}{9},$$
$$\varsigma = 128(-4-2i)^{\frac{2}{3}}\left(\frac{-2+i}{5}\right)^{\frac{1}{3}},$$
$$\Phi = \frac{1}{3}\sqrt{\frac{3-i}{10}}\sqrt{(-4+2i)^{\frac{1}{3}} 15^{\frac{2}{3}} + (27+9i)(-1+m^2+r^2)c_2^2}.$$

The graphical simulations of $u_{4,1}(x,y,z,t)$ are plotted in Figure 5.

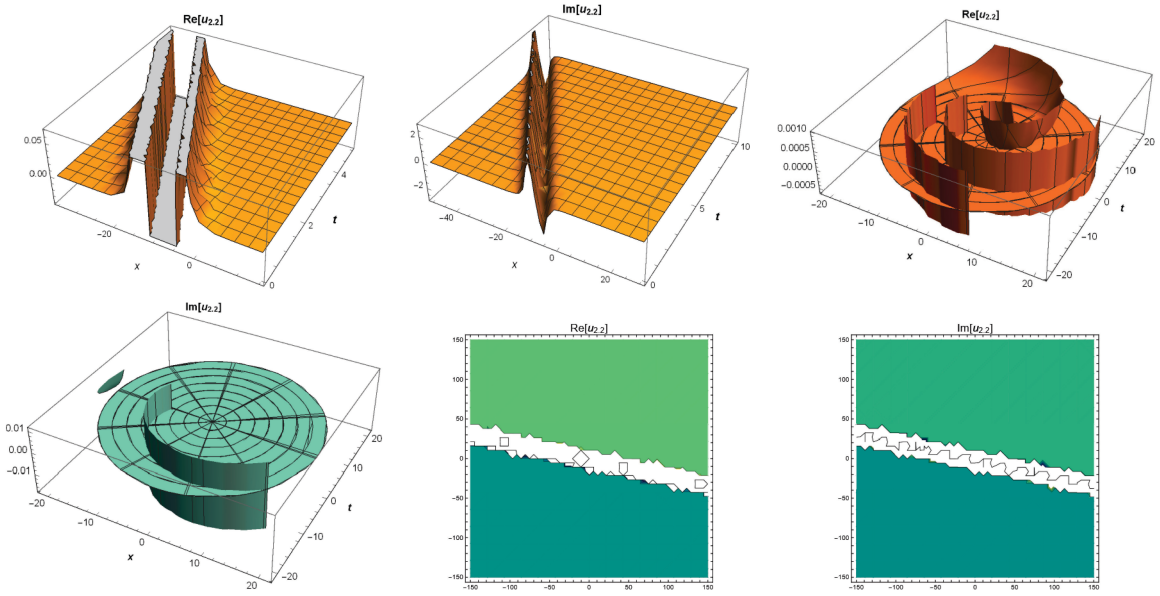

Figure 3. The 3D, revolution and contour surfaces of Eq. (19).

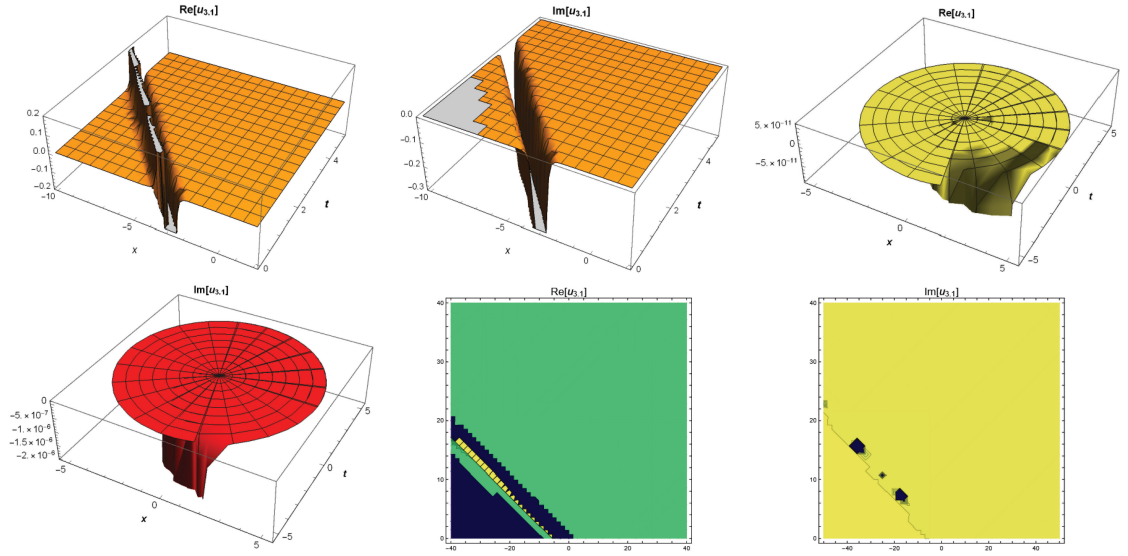

Figure 4. The 3D, revolution and contour surfaces of Eq. (20).

Case 2.2: Under the conditions of Family-4, if we select these conditions,

$$A_3 = i,\ A_1 = A_2 = B_1 = 0,\ \beta = 1,\ n = i,\ \Omega_3 = 1,\ \Lambda_1 = -i,\ \Gamma_1 = 2,\ \Omega_1 = B_0 = 1$$

$$A_0 = \frac{1}{3}\sqrt{1+\frac{i}{2}},\ B_2 = -\left(-\frac{4}{5}+\frac{2i}{5}\right)^{\frac{1}{3}}3^{\frac{2}{3}},\ \alpha = \sqrt{1-2i},\ \lambda = \frac{2(-2)^{\frac{5}{6}}(2+i)^{\frac{1}{6}}}{3^{\frac{1}{3}}},$$

$$r = \frac{1}{3c_1}\left(\sqrt{\frac{-3+i}{10}}\sqrt{(-4+2i)^{\frac{1}{3}}15^{\frac{2}{3}}-(27+9i)k^2+(27+9i)c_1^2(m^2-1)}\right),$$

$$\mu = 2(-2-i)^{\frac{1}{3}}\left(\frac{2}{3}\right)^{\frac{2}{3}},\ \Lambda_2 = \beta^2\Omega_3 - 3\beta^2\Omega_4 + \beta\Gamma_1 + \Lambda_1,\ c_0 = \beta^3(-\Omega_4) - \beta\Lambda_2,$$

$$\Gamma_2 = -3\alpha^2\beta\Omega_4 + 2\alpha^2\beta\Omega_3 + \alpha^2\Gamma_1 - \beta\Omega_2,\ \Omega_4 = \alpha^2\Omega_3 + \Omega_1 - \Omega_2,\ c_1 = c_2$$

we obtain another following complex polynomial solution

$$u_{4,2} = \frac{\frac{1}{3}\sqrt{1+\frac{i}{2}} - \frac{\sigma(mx+iy-kt+\varpi z+E)^3}{\left(4+\frac{4(-2)^{\frac{5}{6}}}{3^{\frac{1}{3}}}(2+i)^{\frac{1}{6}}(mx+iy-kt+\varpi z+E)\right)^3}}{1+\frac{\varepsilon(mx+iy-kt+\varpi z+E)^2}{\left(4+\frac{4(-2)^{\frac{5}{6}}}{3^{\frac{1}{3}}}(2+i)^{\frac{1}{6}}(mx+iy-kt+\varpi z+E)\right)^2}} \quad (23)$$

where

$u_{4,2} = u_{4,2}(x,y,z,t)$, $\sigma = \frac{2048}{9} - \frac{4096i}{9}$,

$\varpi = \frac{1}{3c_2}\left(\sqrt{\frac{-3+i}{10}}\sqrt{(-4+2i)^{\frac{1}{3}}15^{\frac{2}{3}} - (27+9i)k^2 + (27+9i)(-1+m^2)c_2^2}\right)$,

$\Phi = \frac{1}{3}\sqrt{\frac{3-i}{10}}\sqrt{(-4+2i)^{\frac{1}{3}}15^{\frac{2}{3}} - (27+9i)(-1+m^2+r^2)c_1^2}$,

$\varepsilon = 128(-1)^{\frac{1}{3}}\left(\frac{-2+i}{5}\right)^{\frac{1}{3}}\left(\frac{4+2i}{3}\right)^{\frac{2}{3}}$.

The graphical simulations of $u_{4,2}(x,y,z,t)$ are plotted in Figure 6.

DISCUSSIONS

In this section of the paper, we provide two important discussions as follows. Firstly, as one of the trustable methods for extracting various new travelling wave solutions to the double-stranded DNA model, the MEFM has been used. This method is based on the special type of the Riccati differential equation, that is, if we re-consider Eq.(7) as

$$\Omega'(\xi) = e^{-\Omega(\xi)} + \mu e^{\Omega(\xi)} + \lambda \tag{24}$$

together with following equality

$$y = e^{\Omega(\xi)} \tag{25}$$

we can re-write it as below

$$y' = y\Omega'(\xi) \tag{26}$$

and also

$$\Omega'(\xi) = \frac{y'}{y} \tag{27}$$

Putting Eq. (25), Eq. (26), Eq. (27) into Eq.(24) we obtain follows

$$y' = 1 + \lambda y + \mu y^2 \tag{28}$$

Eq (28) is a special type of the Riccati differential equation which needs to be given a special solution. So, in this paper, we consider some special solution parameter, we find several families of the solutions given by second section.

Secondly, if we consider higher values of M and N in Eq. (14), it produces many coefficients to the considered differential equations.[17]. When we consider $M = 3$ and $N = 4$, we write follows:

$$U(\xi) = \frac{A_0 + A_1 e^{-\Omega(\xi)} + A_2 e^{-2\Omega(\xi)} + A_3 e^{-3\Omega(\xi)} + A_4 e^{-4\Omega(\xi)}}{B_0 + B_1 e^{-\Omega(\xi)} + B_2 e^{-2\Omega(\xi)} + B_3 e^{-3\Omega(\xi)}}, \tag{29}$$

where $A_4 \neq 0$ and $B_3 \neq 0$. In Eq.(29), we have two more parameters, such as A_4 and B_3. So, these parameters produce more different traveling wave solutions than the model studied.[18] This is one of the main properties of the method. In this paper, by selecting some of these coefficients, we have obtained some novel complex, exponential, and hyperbolic function solutions to the doublestranded DNA model such as $u_{1.1}$, $u_{2.1}$, $u_{2.2}$, $u_{3.1}$, $u_{4.1}$ and $u_{4.2}$. If we take more values of M and N, we obtain more complicated new analytical solutions for the model studied.

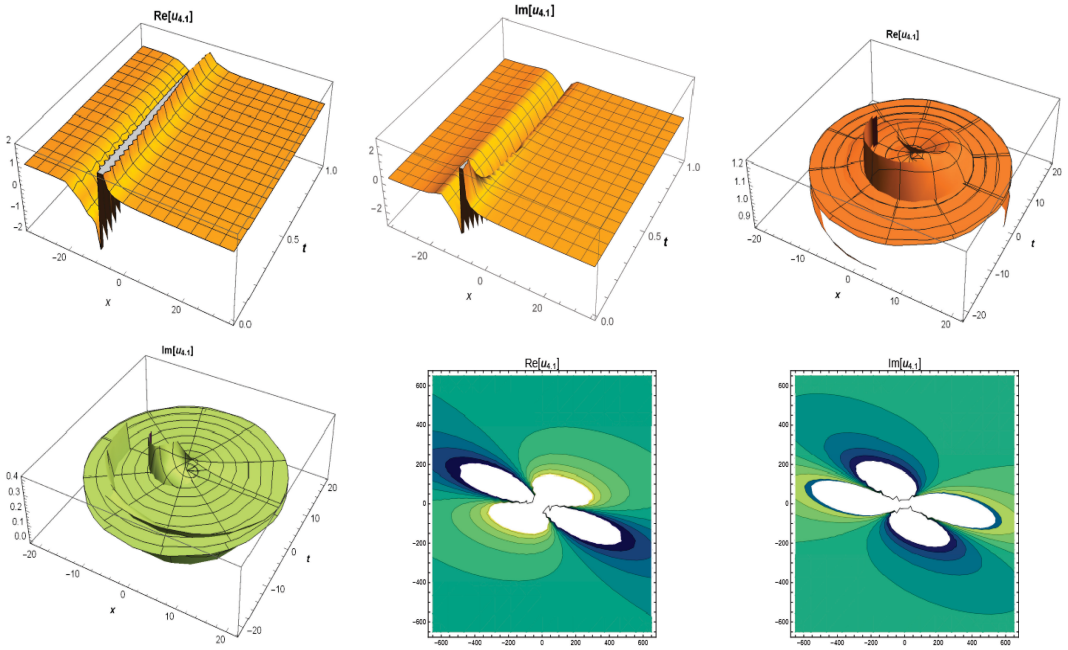

Figure 5. The 3D, revolution and contour surfaces of Eq. (22).

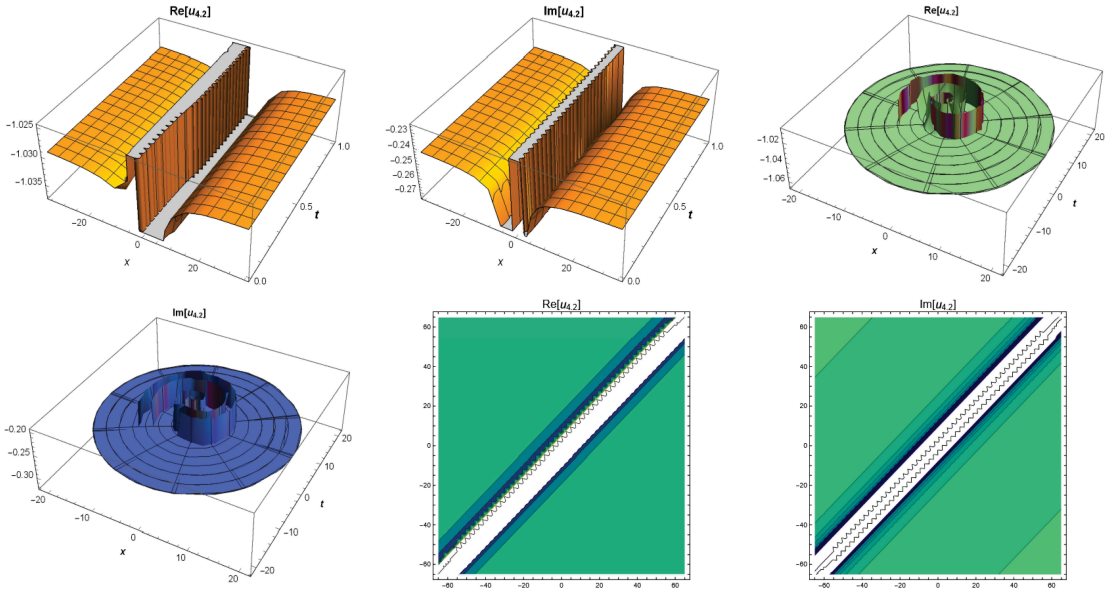

Figure 6. The 3D, revolution and contour surfaces of Eq. (23).

CONCLUSION

In this work, with the aid of computational programs, we have applied MEFM to the double-stranded DNA model. Some new complex polynomial, trigonometric, exponential and hyperbolic function solutions have been reported. All the obtained solutions in this study have verified the considered the doublestranded DNA model given by (1). We have also plotted various dimensional such as 3D, contour and revolution of each obtained solutions. We observed that our solutions are new when compared with the solutions obtained by the existing methods in the literature.[14,19] Via these solutions, it is estimated that these novel solutions may be useful to better understanding of the double-stranded DNA model in various aspects.

Acknowledgment. The research is partially supported by the Fundamental Research Funds for the Central Universities (No. B250201225).

REFERENCES

[1] V. B. Nambiar, B. Ramamurthy, P. Veeresha, *Int. J. Math. Comput. Eng.* **2024**, *2*, 59–70. https://doi.org/10.2478/ijmce-2024-0005

[2] M. Tan, Y. Tan, H. Jiang, J Xue., Q. Wu, Y. Zheng, G. Liu, Y. Xiao, M. Lv, M. Liao, L. Zhang, S. Qu, W. Liang, *Forensic Sci. Int. Genet.* **2025**, *78*, 103289. https://doi.org/10.1016/j.fsigen.2025.103289

[3] M. E. Ozturk, A. A. Tunc, M. F. Akay, *Int. J. Math. Comput. Eng.* **2023**, *1*, 171–176. https://doi.org/10.2478/ijmce-2023-0013

[4] Md. Faruk Hosen, S. M. Hasan Mahmud, K. Ahmed, W. Chen, M. Ali Moni, H.-W. Deng, W. Shoombuatong, Md Mehedi Hasan, *Comput Biol Med.* **2022,** *145*, 105433. https://doi.org/10.1016/j.compbiomed.2022.105433

[5] O. D. Johnson , S. Paul, J. A. Gutiérrez, W. K. Russell, M. C. Ward, *iScience* **2025,** *28*, 112474. https://doi.org/10.1016/j.isci.2025.112474

[6] K. W. Caldecott, *Trends in Cell Biology* **2022**, *32*, 733–745. https://doi.org/10.1016/j.tcb.2022.04.010

[7] M. Ciosi, A. Maxwell, S. A. Cumming, D. J. Moss, A. M. Alshammari, M. D. Flower, A. Durr, B. R. Leavitt, R. A. Roos, P. Holmans, L. Jones, *EbioMedicine* **2019,** *48*, 568–580. https://doi.org/10.1016/j.ebiom.2019.09.020

[8] H. Nikjoo, S. Rahmanian, R. Taleei, *Prog. Biophys. Mol. Biol.* **2024,** *190*, 1–18. https://doi.org/10.1016/j.pbiomolbio.2024.05.002

[9] L. Zagkos, M. Mc Auley, J. Roberts, N. I. Kavallaris, *J. Theor. Biol.* **2019**, *462*, 184–193. https://doi.org/10.1016/j.jtbi.2018.11.006

[10] S. W.Yao, S. M. Mabrouk, M. Inc, A. S. Rashed, *Results Phys.* **2022**, *42*, 105966. https://doi.org/10.1016/j.rinp.2022.105966

[11] K. De-Xing, L. Sen-Yue, Z. Jin, *Commun. Theor. Phys.* **2001**, *36*, 737–742, https://doi.org/10.1088/0253-6102/36/6/737

[12] U. Younas, J. Ren, L. Akinyemi, H. Rezazadeh, *Math. Method Appl. Sci.* **2023**, *46*, 6309–6323. https://doi.org/10.1002/mma.8904

[13] T. S. Hassan, A. A. Elmandouh, A. A. Attiya, A. Y. Khedr, *J. Math.* **2022**, *2022*, 7188118. https://doi.org/10.1155/2022/7188118

[14] S. Kumar, A. Kumar, H. Kharabanda, *Braz. J. Phys.* **2021**, *51*, 1043–1068. https://doi.org/10.1007/s13538-021-00913-8

[15] M. A. Rahman, *Results Phys.* **2014**, *4*, 150–155. https://doi.org/10.1016/j.rinp.2014.07.006

[16] M. A. Abdelrahman, E. H. Zahran, M.M. Khater, *Int. J. Modern Nonlinear Theory Appl.***2015**, *4*, 37–47. https://doi.org/10.4236/ijmnta.2015.41004

[17] H. F. Ismael, H. M. Baskonus, H. Bulut, W. Gao, *Opt. Quantum Electron.* **2023**, *55*, 303. https://doi.org/10.1007/s11082-023-04581-7

[18] K. A. Muhamad, T. Tanriverdi, A. A. Mahmud, H. M. Baskonus, *Int. J. Comput. Math.* **2023**, *100*, 1340–1355. https://doi.org/10.1080/00207160.2023.2186775

[19] H. M. Baskonus, C. Cattani in *Advances in Mathematical Inequalities and Applications* (Eds.: P. Agarwal, S. S. Dragomir, M. Jleli, B. Samet), Springer, Singapore, 2018.